Hindawi
Shock and Vibration
Volume 2017, Article ID 3670769, 14 pages
https://doi.org/10.1155/2017/3670769

Research Article

Dynamic Response Analysis of Cable of Submerged Floating Tunnel under Hydrodynamic Force and Earthquake

Zhiwen Wu and Guoxiong Mei

Key Laboratory of Disaster Prevention and Structural Safety of Ministry of Education, Guangxi Key Laboratory of Disaster Prevention and Structural Safety, College of Civil Engineering and Architecture, Guangxi University, Nanning 530004, China

Correspondence should be addressed to Guoxiong Mei; meiguox@163.com

Received 21 June 2017; Accepted 28 August 2017; Published 15 October 2017

Academic Editor: Hugo Rodrigues

A simplified analysis model of cable for submerged floating tunnel subjected to parametrically excited vibrations in the ocean environment is proposed in this investigation. The equation of motion of the cable is obtained by a mathematical method utilizing the Euler beam theory and the Galerkin method. The hydrodynamic force induced by earthquake excitations is formulated to simulate real seaquake conditions. The random earthquake excitation in the time domain is formulated by the stochastic phase spectrum method. An analytical model for analyzing the cable for submerged floating tunnel subjected to combined hydrodynamic forces and earthquake excitations is then developed. The sensitivity of key parameters including the hydrodynamic, earthquake, and structural parameters on the dynamic response of the cable is investigated and discussed. The present model enables a preliminary examination of the hydrodynamic and seismic behavior of cable for submerged floating tunnel and can provide valuable recommendations for use in design and operation of anchor systems for submerged floating tunnel.

1. Introduction

Submerged floating tunnel is an innovative underwater transportation system to avoid water traffic and weather at a depth of usually 20–50 m. The tunnel floats in water and its position is restrained at a certain distance from the sea bed by means of suitable anchoring systems, such as cables or bars. Cables for submerged floating tunnel are lightweight, very flexible, and lightly damped, the features of which make them particularly prone to vibration. Frequent vibration may lead to fatigue damage of cable, where fatigue cracks could be formed on the cable surface to destroy the anticorrosion system. Eventually the bearing capacity of cable will be lost completely with the propagation of fatigue cracks. The cable for submerged floating tunnel experiences complex dynamic forces under various ocean conditions, which is the key to the safe operation.

Many attentions have been received to the vibration of submerged floating tunnel cables. Sun et al. [1] analyzed the nonlinear response of cables subjected to parametric excitations. Sun and Su [2] investigated the parametric vibration of submerged floating tunnel cable under random excitations. Lu et al. [3] studied the slack phenomenon and the snap force in the cable for submerged floating tunnels under wave conditions. Seo et al. [4] conducted a series of simplified analyses to estimate the behavior of submerged floating tunnel cables in waves and compared their calculations with experimental measurements. Cifuentes et al. [5] implemented a numerical model to analyze the coupled dynamic response of a submerged floating tunnel with mooring lines in regular waves.

It is noted by Duan et al. [6] that 85% of the total amount of earthquakes occurs in the ocean. The Bohai Strait, the Qiongzhou Strait, and the Taiwan Strait in China are three potential areas to build submerged floating tunnels, which are also in the Circum-Pacific seismic belt. Hence, the performance of subsea cables in seismic zones becomes one of the significant academic and engineering attractions

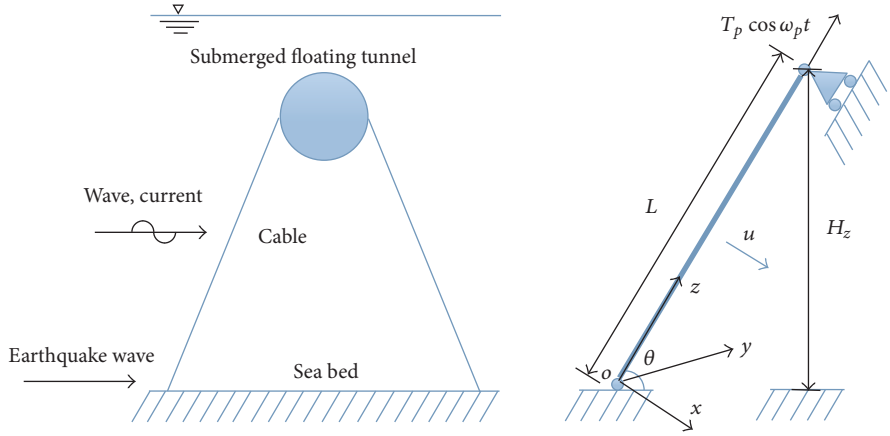

Figure 1: Definition sketch of the submerged floating tunnel model and its cable coordinate system.

in offshore engineering. In addition, the effect of seaquake is much more complex, which can induce hydrodynamic pressures acting on the cable [7, 8]. The combined fluid and seismic motion induced by ocean hydrodynamic forces must be considered rigorously in the analysis of cables for submerged floating tunnel during earthquakes. Therefore, it is of significance to evaluate how parametrically excited vibrations influence the behavior of cable for submerged floating tunnel under combined hydrodynamic force and earthquake.

Although earthquakes have significant effect on the performance of cables for submerged floating tunnel, few studies have been reported to assess the seismic response of cables except those from [9–11]. In these previous studies, the effects of earthquake on the development of hydrodynamic force were usually neglected, and the seismic design spectrum was taken from design guidelines for buildings (e.g., the Chinese code for seismic design of buildings (GB 50011-2010) [12] directly). However, the seismic design spectrum for buildings is not always suitable for marine structures, the distinctiveness of marine site classifications of offshore structures in marine environment cannot be considered, and the correctness of this approach becomes questionable.

The present study aims to establish a mathematical method to explore the dynamic response of cable for submerged floating tunnel under simultaneous hydrodynamic forces and earthquake excitations. A simplified analysis model to estimate the behavior of cable for submerged floating tunnel under the ocean environmental excitation is proposed. The equation of motion of the cable is obtained by a mathematical method utilizing the Euler beam theory and the Galerkin method. The hydrodynamic force induced by earthquake excitations is formulated to simulate real seaquake conditions. The random earthquake force in the time domain is calculated by the stochastic phase spectrum method. An analytical model for analyzing the cable for submerged floating tunnel subjected to combined hydrodynamic forces and earthquake excitations is then developed. The sensitivity of key parameters including the hydrodynamic, earthquake, and structural parameters on the dynamic response of the cable is investigated and discussed.

2. Method

2.1. Equation of Motion for the Cable. Following previous studies [1, 3, 11, 13], a simplified analysis model is proposed to evaluate the motion of cables for submerged floating tunnel subjected to ocean environmental excitations. For simplification, the cable for submerged floating tunnel is modeled as a Bernoulli-Euler beam, which only allows the in-plane motion of the cable. Furthermore, a conservative assumption is adopted that the response of the cable under combined effects of hydrodynamic forces and earthquake excitations is maximized when the two actions are in the same direction. A submerged floating tunnel and the direction of earthquake wave and wave/current force are schematically shown in Figure 1, where the cable is allowed to move only in the inline direction. It should be emphasized that the horizontal earthquake excitation is acting on the anchoring point of the cable.

Figure 1 shows the schematic illustration of a submerged floating tunnel and cable. In this simplified analysis model, the three-dimensional behavior is not taken into consideration. Although this assumption simplifies the physical phenomenon, the two-dimensional model enables a preliminary examination of the hydrodynamic and seismic behavior of cables. The origin of the coordinate system is set at the anchored point of the cable on the sea bed. The parameter L is the undeformed length of the cable, H_z shows the vertical height above the sea bed, u represents the dynamic displacement at the mid-span of the cable, and θ denotes the inclination angle of the cable with respect to the sea bed.

The effect of the tunnel tube on the cable is simplified as a parametric excitation $T_p \cos \omega_p t$, and the ends of the cable are hinged [2, 14], where T_p is the dynamic tension acting on the cable induced by the motion of the tube, and ω_p is the parametric excitation frequency. For simplicity, the initial tension, geometry, stiffness, and material property of the cable are assumed to be constant along the cable length.

Thus, the governing equation of the motion of the cable can be written as [2, 3, 11, 13]

$$E_{\text{eq}}I\frac{\partial^4 u(z,t)}{\partial z^4} - \frac{\partial}{\partial z}\left(T_0 + T_p\cos\omega_p t\right)\frac{\partial u(z,t)}{\partial z} + m\frac{\partial^2 u(z,t)}{\partial t^2} + C_s\frac{\partial u(z,t)}{\partial t} = F_L - F_D - Q_s\sin\theta, \quad (1)$$

where $u(z,t)$ is the dynamics lateral displacement of cable, T_0, m, E_{eq}, and I are the initial tension, mass per unit length, the equivalent modulus of elasticity, and the cross-sectional moment of inertia of the cable, respectively, C_s is the viscous damping coefficient, F_L is the vortex-induced lift force, F_D is the acting drag force applied by water per unit length when the cable oscillates, and Q_s is the earthquake excitation force.

While considering the cable sag effect, the equivalent elastic modulus of cable can be obtained by the following equivalent method [11]:

$$E_{\text{eq}} = \frac{E}{\left(1 + E/E_f\right)}, \quad E_f = \frac{12\sigma^3}{\left[\gamma_1^2\left(L\cos\theta\right)^2\right]}, \quad \sigma = \frac{T_0}{A_c}, \quad (2)$$

where E is the modulus of elasticity of cable, E_f is the modulus of elasticity induced by sag of cable, γ_1 is the buoyant unit weight of the cable, σ is the stress of cable, and A_c is the cross-sectional area of cable.

2.2. Earthquake Excitation in the Time Domain. The earthquake excitation in the time domain can be expressed as

$$Q_s = m\ddot{x}_g, \quad (3)$$

where $\ddot{x}_g$ is the acceleration of the input ground motion, which can be derived from the earthquake records obtained from seismic stations at a given location or from an artificial stochastic process using the trigonometric series method.

Since the random excitation of earthquakes is transient, the nonstationary characteristics of random excitation should be considered. Using the evolutionary theory of power spectrum density [15], the nonstationary random process can usually be written as the product of a stationary random process and a deterministic slowly varying modulation function

$$\ddot{x}_g = a(t)\,w(t), \quad (4)$$

where $a(t)$ is a stationary process and $w(t)$ is the deterministic envelope function with a maximum value of 1.0.

The deterministic envelope function $w(t)$ is written as [10]

$$w(t) = \begin{cases} \left(\dfrac{t}{t_0}\right)^2 & 0 < t < t_0 \\ 1 & t_0 < t < t_n \\ \exp\left[-c\left(t - t_n\right)\right] & t_0 < t, \end{cases} \quad (5)$$

where t_0 and t_n are the initial time and the nth time, respectively, $t_0 - t_n$ is the significant duration of the accelerogram, and c is the nonuniformly modulated coefficient. A typical value of c is adopted as 0.2.

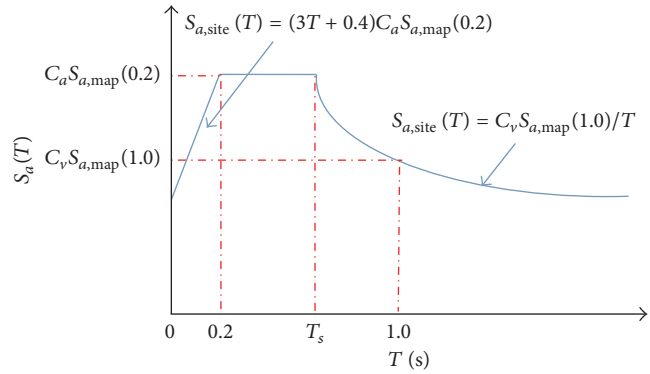

FIGURE 2: ISO seismic design spectrum.

A possible approach to define $a(t)$ is by assuming that the motion induced by earthquakes is a realization of a stationary stochastic process. The time history of a stationary earthquake excitation can be readily generated based on the spectral density as follows:

$$a(t) = \sum_{k=1}^{n}\sqrt{\left(4\cdot\Delta\omega\cdot S\left(\omega_k\right)\right)}\cos\left(\omega_k t + \varepsilon_k\right), \quad (6)$$

where $\Delta\omega$ is the constant difference between successive frequencies, $\omega_k = k\cdot\Delta\omega$ is the kth wave frequency, $S(\omega_k)$ is the power spectrum of ω_k, n is the total number of frequency points considered in the calculation, and ε_k is the random phase angle varying between 0 and 2π.

In engineering practice [15], the design target response spectrum at a given site is more commonly available than the ground motion power spectrum density function. Therefore, it will be very useful to generate time histories of ground motion that are compatible to a given design target response spectrum.

The design target acceleration response spectrum $S_a^T(\omega)$ can be obtained in seismic design guidelines, which cannot be directly used by (6). Thus, a conversion formula is needed to obtain the corresponding ground motion power spectrum $S(\omega)$.

For a given design target acceleration response spectrum $S_a^T(\omega)$, the corresponding ground motion power spectrum $S(\omega)$ can be estimated by [15]

$$S(\omega) = \frac{\zeta}{\pi\omega}\left[S_a^T(\omega)\right]^2\frac{1}{\ln\left[-\left(\pi/\omega T_d\right)\ln\left(1-P\right)\right]}, \quad (7)$$

where T_d is the time duration of earthquake, ζ is the damping ratio, and P is the exceeding probability. In the present study, the value of the parameter P is taken as 0.9.

The design target acceleration response spectrum is normally determined by basic parameters of seismic intensity, site classification, peak acceleration, and damping ratio. The seismic design spectrum curve as shown in Figure 2 can be found in the ISO design guidelines (ISO, 2006) [16]. In the figure, S_a is the spectral acceleration, $S_{a,\text{site}}(T)$ is the site spectral acceleration, and $S_{a,\text{map}}$ is the bedrock spectral acceleration. When the fundamental period of a structure is

equal to 0.2 or 1.0 s, the bedrock spectral acceleration can be calculated by $S_{a,\mathrm{map}}(0.2) = 0.5g$ or $S_{a,\mathrm{map}}(1.0) = 0.2g$. The parameter T is the fundamental period of the structure, and T_s is the site characteristic period and can be calculated as follows:

$$T_s = \frac{C_v S_{a,\mathrm{map}}(1.0)}{C_a S_{a,\mathrm{map}}(0.2)}, \tag{8}$$

where C_a and C_v are the site coefficients and can be obtained from the design tables in ISO (2006) [16].

Assuming that the submerged floating tunnel investigated in this paper is located in the Bohai Sea of China with anchoring systems on a shallow foundation, the site class of the foundation is categorized as A. For a site class A/B and a shallow foundation, the parameters C_a and C_v are both assigned as 1.0.

Using the above approach, the generated time histories of ground motion usually match well with the design target response spectrum. Iterations should be carried out to adjust the power spectrum density function if the two spectra do not match satisfactorily [15].

2.3. Formulation of Hydrodynamic Force in Time Domain. The vortex-induced lift force can be expressed as [17]

$$F_L = \frac{1}{2}\rho_w D C_L \left(v_L \sin\theta\right)^2 \sin\left(\omega_v t\right), \tag{9}$$

where ρ_w is the water density, D is the outer diameter of the cable, ω_v is the vortex shedding frequency, C_L is the vortex-induced lift coefficient, and v_L is the vortex flow velocity and its typical value is taken as 1.0 m/s.

The hydrodynamic force F_D can be expressed by Morison's equation [14] as follows:

$$\begin{aligned} F_D = {} & \frac{1}{2}\rho_w D C_D \left(v - \frac{\partial u}{\partial t}\right)\left|v - \frac{\partial u}{\partial t}\right| + C_M \frac{\pi}{4}\rho_w D^2 \frac{\partial v}{\partial t} \\ & - \left(C_M - 1\right)\frac{\pi}{4}\rho_w D^2 \frac{\partial^2 u}{\partial t^2}, \end{aligned} \tag{10}$$

where C_D is the drag coefficient, C_M is the inertia coefficient, u is the displacement of the cable, and v is the instantaneous current velocity.

The hydrodynamic force induced by earthquake excitation is formulated following four assumptions [7, 18, 19].

(1) As the earthquake excitation process is in a short time duration, the current velocity around the cable during earthquakes is assumed to be negligible.

(2) When the ground motion is horizontal, the current velocity is set as zero; when the ground motion is vertical, the current velocity is equal to the ground velocity.

(3) The wave force is neglected as the cable is located in deep water.

(4) The coupled effect between the motions in different directions is neglected.

Thus, the hydrodynamic force under earthquake excitation can be expressed by [7, 18, 19]

$$\begin{aligned} F_D = {} & \frac{1}{2}\rho_w D C_D \left(\dot{x}_g - \frac{\partial u}{\partial t}\right)\left|\dot{x}_g - \frac{\partial u}{\partial t}\right| \\ & + C_M \frac{\pi}{4}\rho_w D^2 \ddot{x}_g - \left(C_M - 1\right)\frac{\pi}{4}\rho_w D^2 \frac{\partial^2 u}{\partial t^2}. \end{aligned} \tag{11}$$

2.4. Solution of the Equation. Suppose that the oscillation mode of the cable is that of standard chord

$$u(z,t) = \sum_{n=1}^{\infty} \sin\frac{n\pi z}{L} u_n(t). \tag{12}$$

To obtain an approximate solution of (1), Galerkin method is applied to transform the partial differential equation into a set of ordinary ones.

Substituting (12) into (1), multiplying each term by $\sin(n\pi z/L)$, integrating over $z \in (0, L)$, and invoking the orthogonality property of the normal modes give

$$\begin{aligned} & \ddot{u}_n + \left[\omega_{Mn}^2 + \omega_{An}^2\left(1 + \varepsilon\cos\omega_p t\right)\right] u_n + \frac{C_{sn}}{m}\dot{u}_n \\ & - \int_0^L \frac{2\left(F_L - F_D - Q_s\sin\theta\right)}{mL}\sin\frac{n\pi z}{L}dz = 0 \end{aligned} \tag{13}$$

with

$$\omega_{Mn}^2 = \left(\frac{n\pi}{L}\right)^4 \frac{E_{\mathrm{eq}} I}{m}, \tag{14}$$

$$\omega_{An}^2 = \left(\frac{n\pi}{L}\right)^2 \frac{T_0}{m}, \tag{15}$$

$$\omega_n = \sqrt{\omega_{Mn}^2 + \omega_{An}^2}, \tag{16}$$

$$C_{sn} = 2m\omega_n\zeta, \tag{17}$$

where ζ is the damping ratio of the cable, ω_{Mn}, ω_{An} are the nth order natural frequency of the system of bending vibration and axial vibration, respectively, ω_n is the total nth order natural frequency of the system, and ε is the ratio of dynamic tension to static tension.

The fourth-order Runge-Kutta method is used to solve the differential equation (13); each mode response of the cable under excitation may be obtained. By substituting the mode response into (12), the displacement response of the cable may be obtained.

3. Numerical Results and Discussion

The cable of a submerged floating tunnel is analyzed in the present study as an illustrative example to show the efficacy of the proposed analytical solution that is programmed in MATLAB. The physical and geometric parameters are listed in Table 1 following the work of Sun and Su [2]. If the same values of $C_M = 1.0$ and $C_D = 0.7$ provided by Sun and Su [2] are used, it can result in the loss of hydrodynamic added

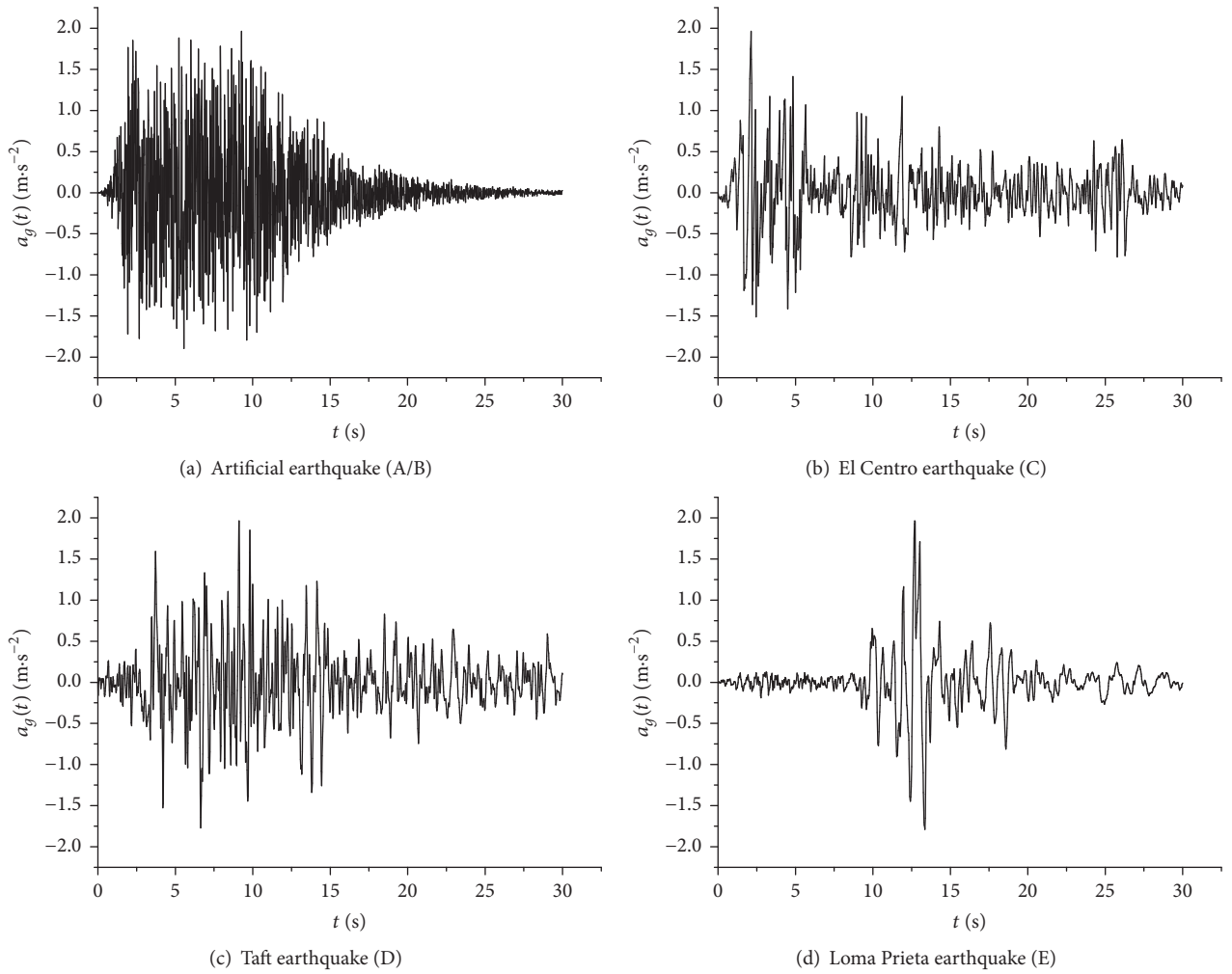

Figure 3: Time histories of four selected earthquake records.

Table 1: Basic characteristics of the analysis case.

Parameters	Values
Density of water ρ_w (kg/m^3)	1028
Depth of water d (m)	170
Vertical height H_z (m)	140
Unstretched length of cable L (m)	161.66
Outside diameter of cable D (m)	0.489
Density of cable ρ_s (kg/m^3)	7850
Modulus of elasticity of cable E (Pa)	2.10E11
Initial tension of cable T_0 (N)	2.572E7
Mass per unit length of cable m (kg/m)	1474.23
Damping ratio ζ	0.0018
Inertia coefficient C_M	2.0
Drag coefficient C_D	1.0
Inclination angle θ (°)	60

mass. Thus, the values of C_M and C_D are taken as 2.0 and 1.0, respectively, following the work of Martire et al. [20].

In the present study, four earthquake records in different representative sites are selected. For comparison, the peak acceleration of these accelerograms is adjusted to $0.2g$, corresponding to earthquakes with an intensity factor of 8 as shown in Figure 3 and Table 2 [16, 21].

The artificial earthquake is generated by using the aforementioned theory in Section 2.2, and the other three earthquakes are the classical earthquake records obtained from corresponding site classifications. The time histories in time domain, the amplitude, and energy in frequency domain of four earthquakes are different, matching different site classifications.

A sensitivity analysis is conducted to evaluate the influence of key parameters to provide recommendations for use in design and construction of the anchor system for a submerged floating tunnel under hydrodynamic force and earthquake. The effects of key environmental and structural

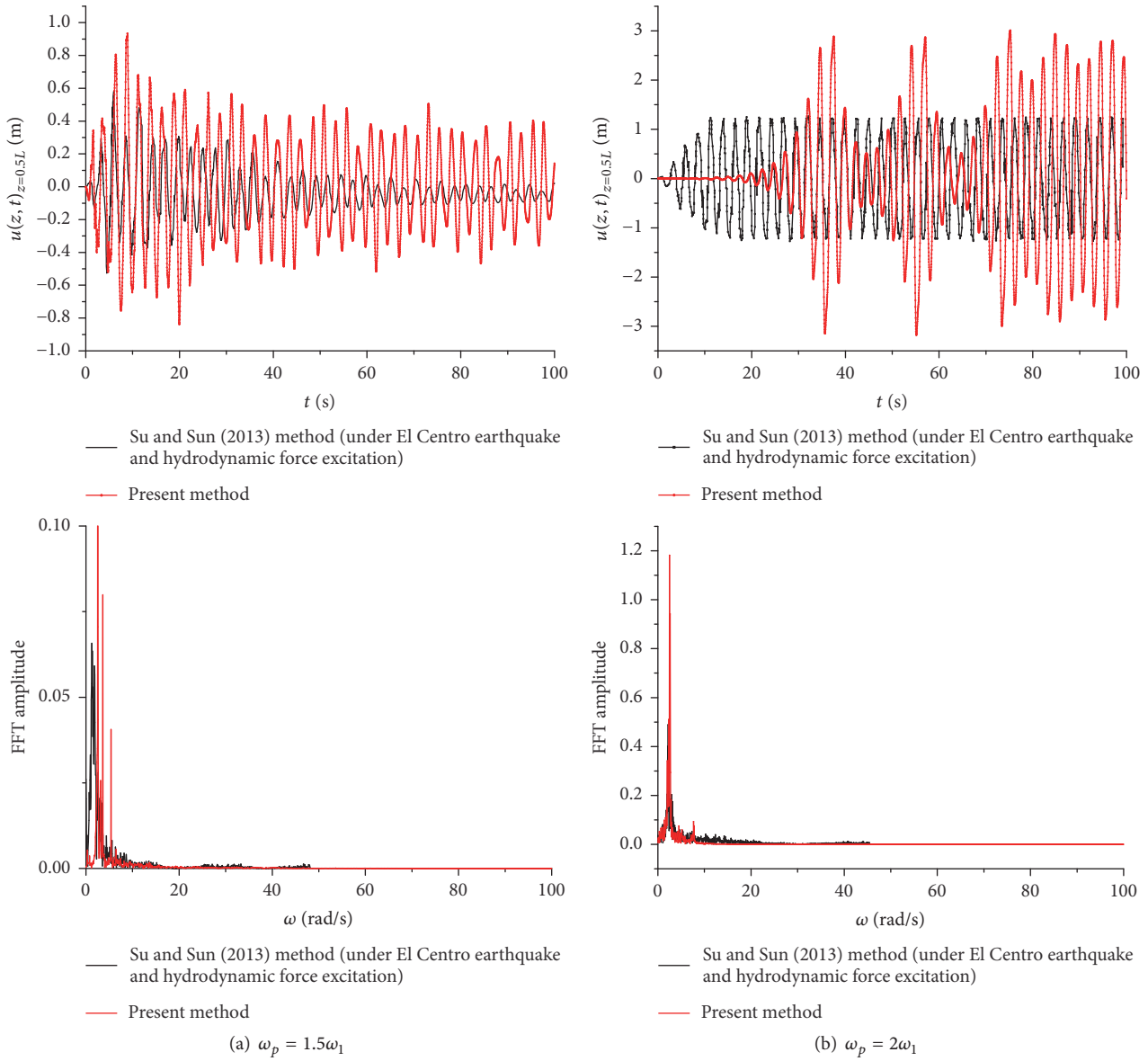

Figure 4: Mid-span displacement of the cable subjected to El Centro earthquake.

parameters on the dynamic responses of the cable for submerged floating tunnel are investigated.

3.1. Evaluation of the Proposed Method. In order to evaluate the effectiveness of the developed method, results evaluated using the developed approach are compared with those calculated using the method of Chen et al. (2008) [22] and Su and Sun (2013) [11].

In Figure 5, the overall trends of the results obtained by the present method generally agree with the evaluations calculated from the other methods. The present method captures the peak value well at resonance condition (i.e., $\omega_p/\omega_1 = 1, 2$), as well as the subsequent attenuation trend. Overall, the calculation by the present method is acceptable and reasonable.

In Figures 4 and 5, the dynamic responses of the cable under hydrodynamic force and earthquake excitation can be greatly amplified by the present method. Especially under the super-resonance condition (i.e., $\omega_p/\omega_1 = 2$), it can be observed that the FFT amplitude component obtained by the present method has more abundant high-frequency contents and excites wider peak frequency region than that of those calculated using the method of Su and Sun (2013). A possible explanation for the difference in calculations could be due to the reason that the seismic design spectrum for marine geotechnical geology is used in the present approach, which is more reasonable and accurate than other strategies by using seismic design spectrum for overland building. Another possible explanation could be the fact that the coupled effect of hydrodynamic force and earthquake excitation is

Table 2: Site classifications of earthquake records used for this study.

Ground motion	Site classifications	Site condition	Time duration (s)	Time interval (s)
Artificial earthquake	A/B	Rock	30	0.02
El Centro earthquake in the EW direction	C	Very dense hard soil and soft rock	30	0.02
Taft Kern County (Taft for short) earthquake in the N21E direction	D	Stiff to very stiff soil	30	0.02
Loma Prieta Oakland outer wharf (Loma for short) earthquake	E	Soft soil	30	0.02

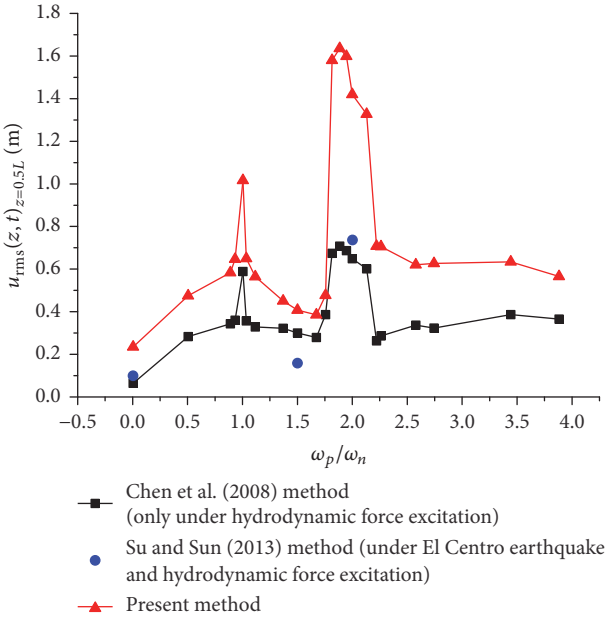

Figure 5: Variations of RMS of mid-span displacement of the cable with ω_p/ω_n calculated using different methods.

incorporated in the present approach, while this coupled effect and the hydrodynamic added mass are neglected in other strategies. Similar results of underestimation by the existing analytical models [11, 22] compared to experimental measurements and numerical simulations were reported [8, 19].

3.2. Dynamic Response of the Cable under Only Vortex Excitation. Vortex-induced vibration of cables is caused by complex interactions between cylindrical structures and the correlated wake vortex, and it is an important source of fatigue damage to the cables. Figure 6 shows the dynamic response of the cable under only vortex excitation. Two cases are investigated in which no oscillation was excited by vortex-shedding in type of $\omega_v = 0.1\omega_1$ and vortex-induced vibration in type of $\omega_v = \omega_1$, which are showed in Figures 6(a) and 6(b) respectively. In Figure 6(a), the dynamic response of the cable shapes as a sinusoidal curve and its amplitude is small. And, in Figure 6(b), the action of exciting system to vibrate will happen as the lift force falls into the lock-in range; that is, beat phenomenon obviously occurs. Besides, due to the self-limitation of damping, the time history of vortex-induced vibration shown in Figure 6(b) decreases rapidly in the first 200 s, but the decreasing pattern is roughly linear and reaches a steady-state response quickly. And it can be observed that the amplitude of dynamic responses of the cable in the condition of lock-in case $\omega_v = \omega_1$ is signally larger than the other case of $\omega_v \neq \omega_1$. Figure 6(c) shows similar results; the largest dynamic response occurs when vortex-induced frequency is consistent with the structural natural frequency; that is, $\omega_v = \omega_1$. Besides, the value of dynamic response of the cable in the other frequency is relatively small.

3.3. Dynamic Response of the Cable under Combinations of Vortex Excitation and Parametric Excitation. In practice, for the cable of submerged floating tunnel suffering both parametric excitation and vortex excitation, its structural configuration is more complex rather than merely an Euler beam alone. Moreover, it is more complicated if two excitation frequencies of both top-end tube and vortex-induced lift force are involved.

Figures 7(a)–7(d) show four typical examples of the cable under combinations of vortex excitation and parametric excitation, and these dynamic responses exhibit interesting and different features of the pattern and shape of the time history. In Figure 7(c), a combined resonance occurs owing to both parametric excitation and vortex-shedding excitation, where both excitations satisfy the condition that can excite resonance of a system under only parametric or vortex shedding excitation, and its motion amplitude is obviously larger and more unstable than those of the other cases in Figures 7(a), 7(b), and 7(c). Figure 7(a) shows the time history of the cable when in case of $\omega_v = \omega_1$ and $\omega_p = 0.1\omega_1$, as vortex excitation dominates parametric excitation, beat phenomenon still occurs in this case and has the smallest motion amplitude. In Figures 7(b) and 7(d), as parametric excitation dominates vortex excitation, beat phenomenon is broken in those cases, the pattern of each time history is a kind of "standing wave," where each has a repeating wave-unit but with mutually different profiles, and the number of wave-units is approximatively ranging from 2.5 to 3.5 and the profiles become more irregular. Therefore, it can be concluded that the dynamic response of the cable under combinations of vortex excitation and parametric excitation became more complicated, especially in combined resonance condition.

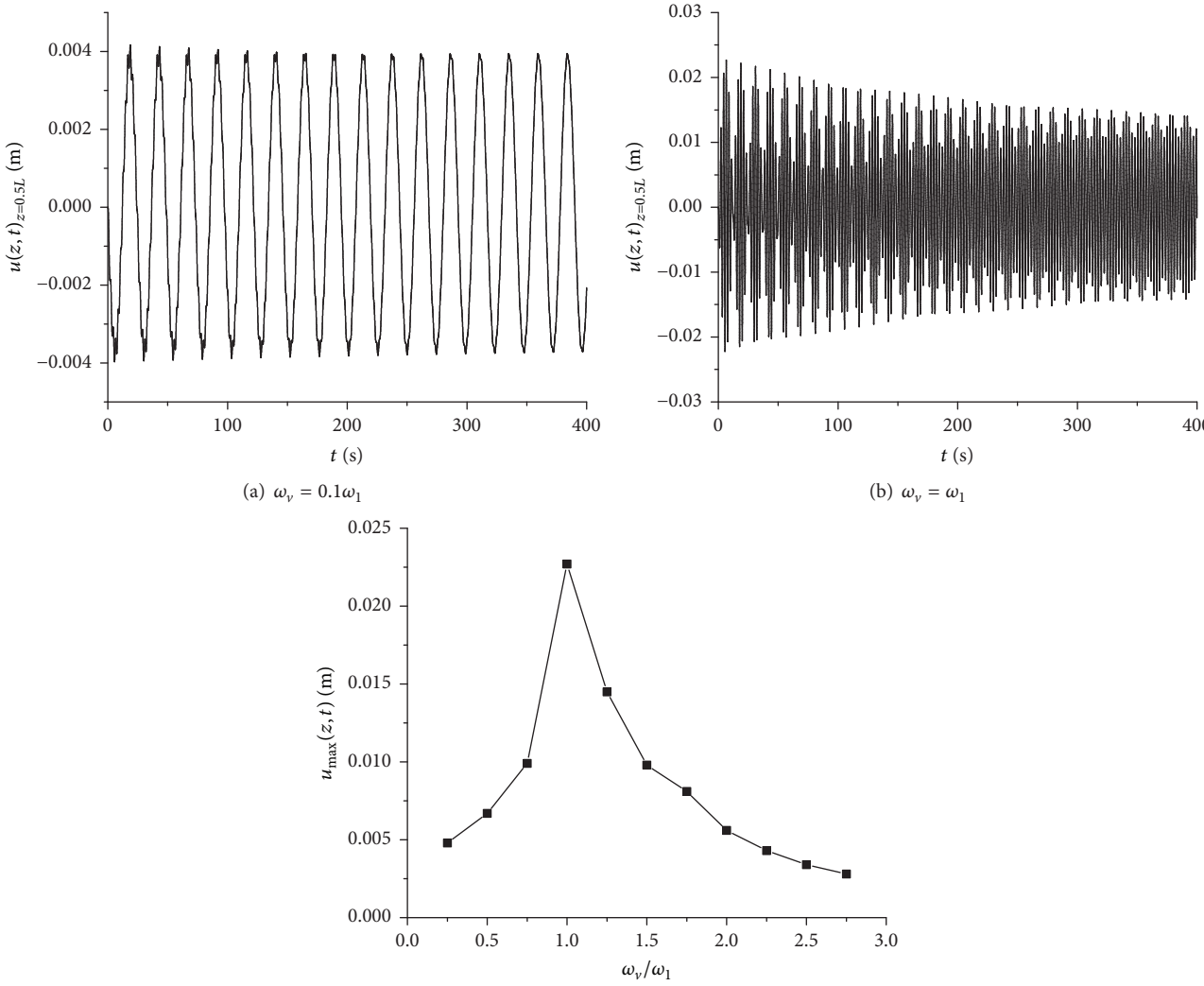

(a) $\omega_v = 0.1\omega_1$

(b) $\omega_v = \omega_1$

(c) Maximum displacement versus ω_v/ω_1

Figure 6: Dynamic response of the cable under only vortex excitation.

Figure 7(e) indicates that three largest amplitudes of dynamic response are, respectively, at the ratio of parametric frequency to natural frequency of $\omega_p/\omega_1 = 1, 2,$ and 3, and the peak values of the mid-span displacement of the cable under above cases are 0.4013 m, 0.8914 m, and 0.2891 m, respectively. Particularly, the largest response amplitude occurs at frequency $\omega_p/\omega_1 = 2$. Or, we may say, for mode 1, the largest dynamic response might occur when top-end tube parametric frequency is twice as much as the natural frequency; that is, $\omega_p = 2\omega_1$ when parametric excitation satisfies the condition which can excite parametric resonance of a system under parametric excitation. Besides, the value of dynamic response of the cable in the other frequency case is relatively small. The results suggest that parametric excitation has a strong effect on the dynamic response of the cable, especially combined with vortex shedding frequency consistent with the structural natural frequency; that is, $\omega_v = \omega_1$.

Thus, the fundamental frequency of cable of submerged floating tunnel located in complicated marine environment should be thought over carefully to avoid parametric resonance. Based on (14)–(16), the key parameters for deciding the fundamental frequency of the cable are m, E_{eq}, I, T_0, and L, while the parametric excitation frequency ω_p mainly depends on ocean environmental conditions acting on the tube.

3.4. Effect of Motion of Top-End Tube. The comparison of modal dynamic responses between the cases with top-end tube moving and without top-end tube moving is presented in Figure 8. The dynamic responses of the cable are numerically simulated, while the top-end tube is moving at the cable's natural frequencies of modes ranging from mode 1 to mode 12, and the most dangerous cases are taken into account; that is, $\omega_v = \omega_j$ and $\omega_p = 2\omega_j$; here, ω_j is the j model natural frequency. In Figure 8, as modal number increases, the cable's

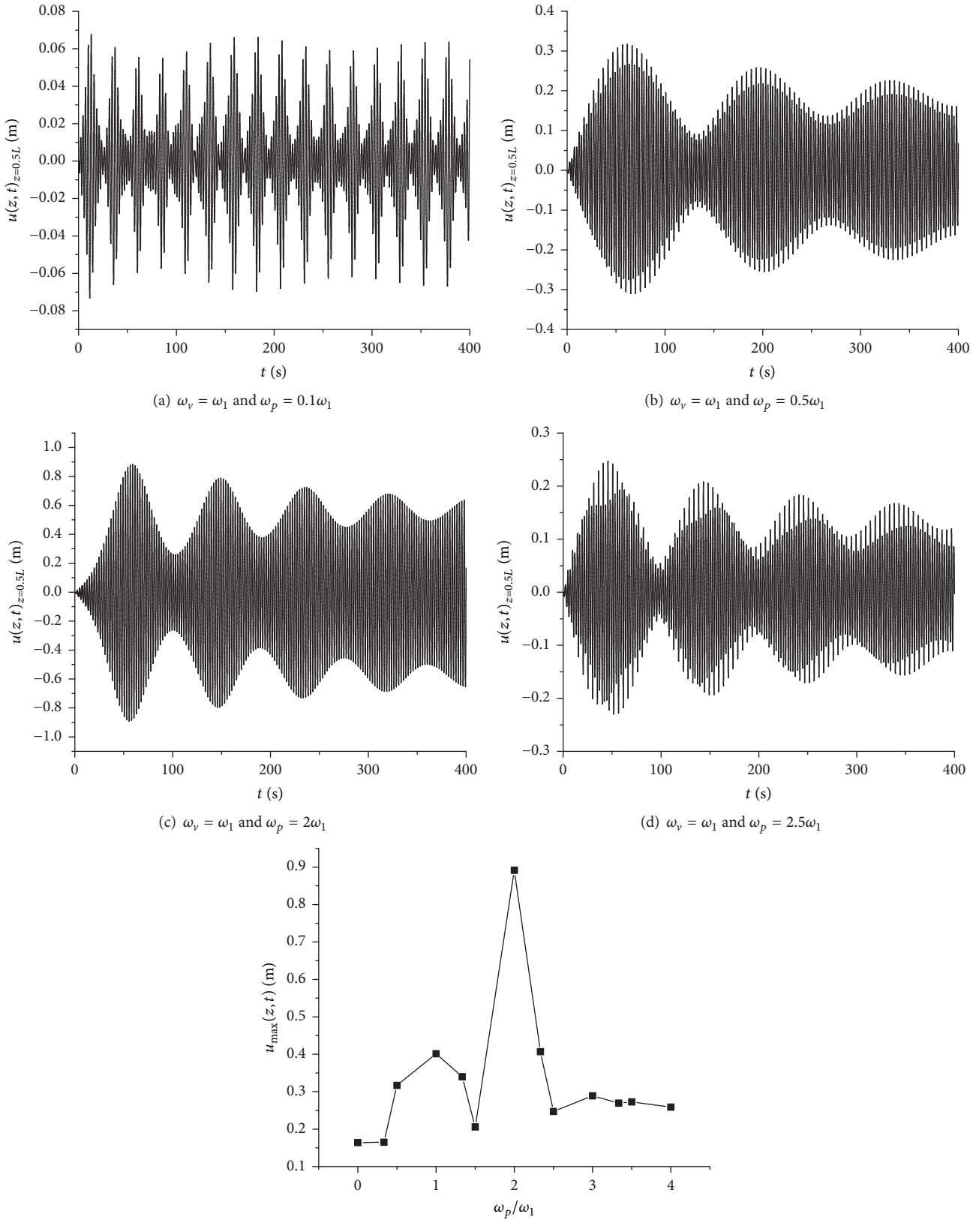

(a) $\omega_v = \omega_1$ and $\omega_p = 0.1\omega_1$

(b) $\omega_v = \omega_1$ and $\omega_p = 0.5\omega_1$

(c) $\omega_v = \omega_1$ and $\omega_p = 2\omega_1$

(d) $\omega_v = \omega_1$ and $\omega_p = 2.5\omega_1$

(e) Maximum displacement versus ω_p/ω_1

Figure 7: Dynamic response of the cable under combinations of vortex excitation and parametric excitation.

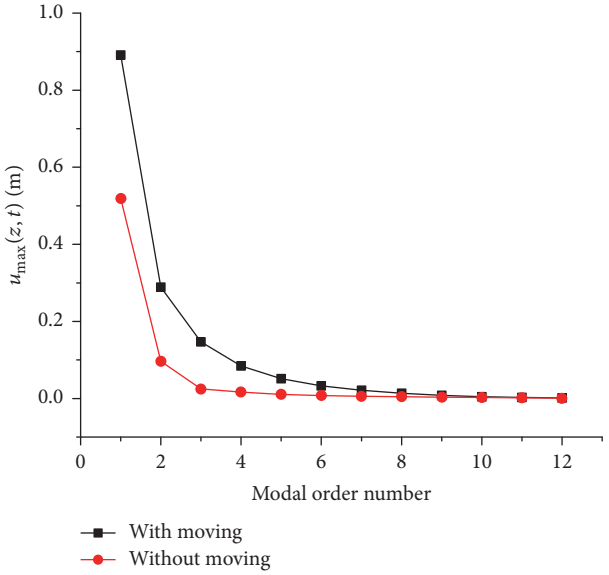

Figure 8: Comparison of modal dynamic responses between the cases with top-end tube moving and without top-end tube moving.

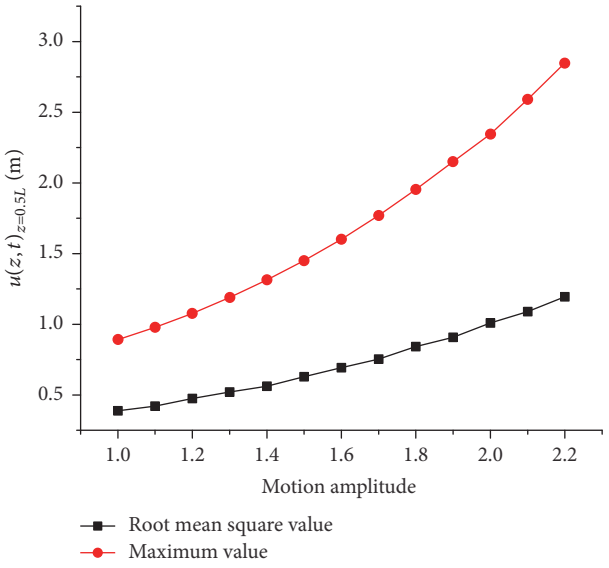

Figure 9: The effect of motion amplitude of top-end tube on the dynamic response of the cable.

vibration either with top-end tube moving or without top-end tube moving attenuates rapidly to small value, even zero. It is noted that the first third-order mode responses are mostly dominated, and they take up more than 80% of the whole mode response. Also, it is shown that the maximum amplitudes of the cable with top-end tube moving are larger than the cases without top-end tube moving, and taking mode 1 as an example, its maximum amplitude is about twice larger than the case without top-end tube moving.

Figure 9 shows the curves of the maximum value and root mean square value of the dynamic response of the cable as the motion amplitude of top-end tube varies from 1.0 to

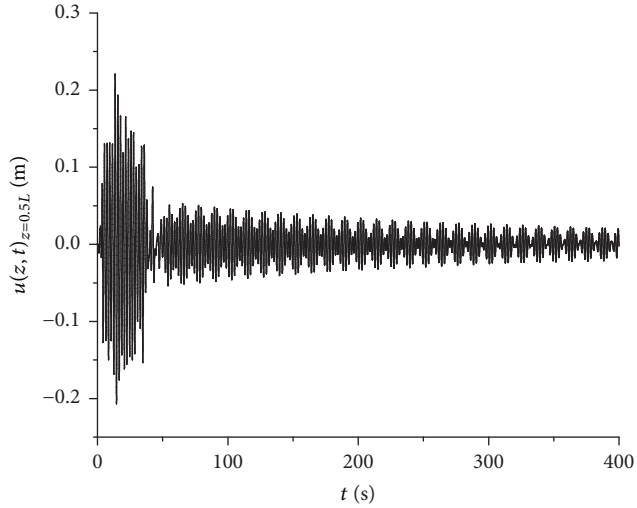

(a) $\omega_v = \omega_1, \omega_p = 0.0\omega_1$ and under Taft earthquake

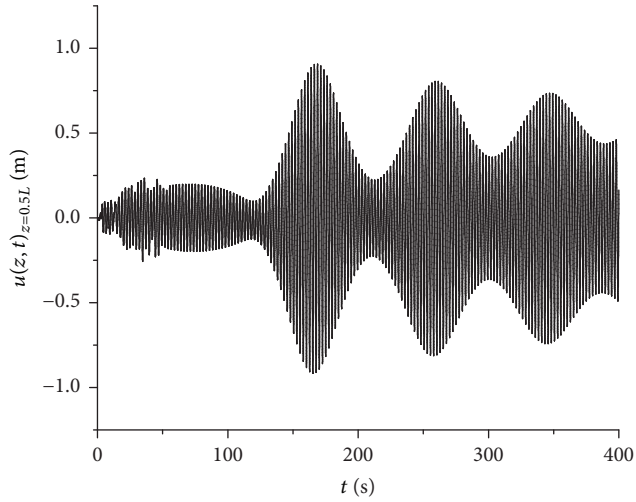

(b) $\omega_v = \omega_1, \omega_p = 1.0\omega_1$ and under Taft earthquake

Figure 10: The effect of earthquake on the dynamic response of the cable.

2.2, where motion amplitude is expressed by the ratio of dynamic tension to static tension ε. In both the two cases, the variational laws of curves are similar, and the maximum value of the displacement increases with the increase of motion amplitude, which is very dangerous for the cable system. And, the root mean square value of the dynamic response of the cable rises almost linearly with the increase of motion amplitude. Thus, motion amplitude of top-end tube is the most important parameter in determining the dynamic response of the cable which necessitates careful consideration during the early stage of design.

3.5. Effect of Earthquake. Figure 10 shows the dynamic response time history of the cable when in combinations of vortex excitation and parametric excitation under Taft earthquake. When the cable is subjected to the earthquake, the maximum value and the mean value in this case are signally

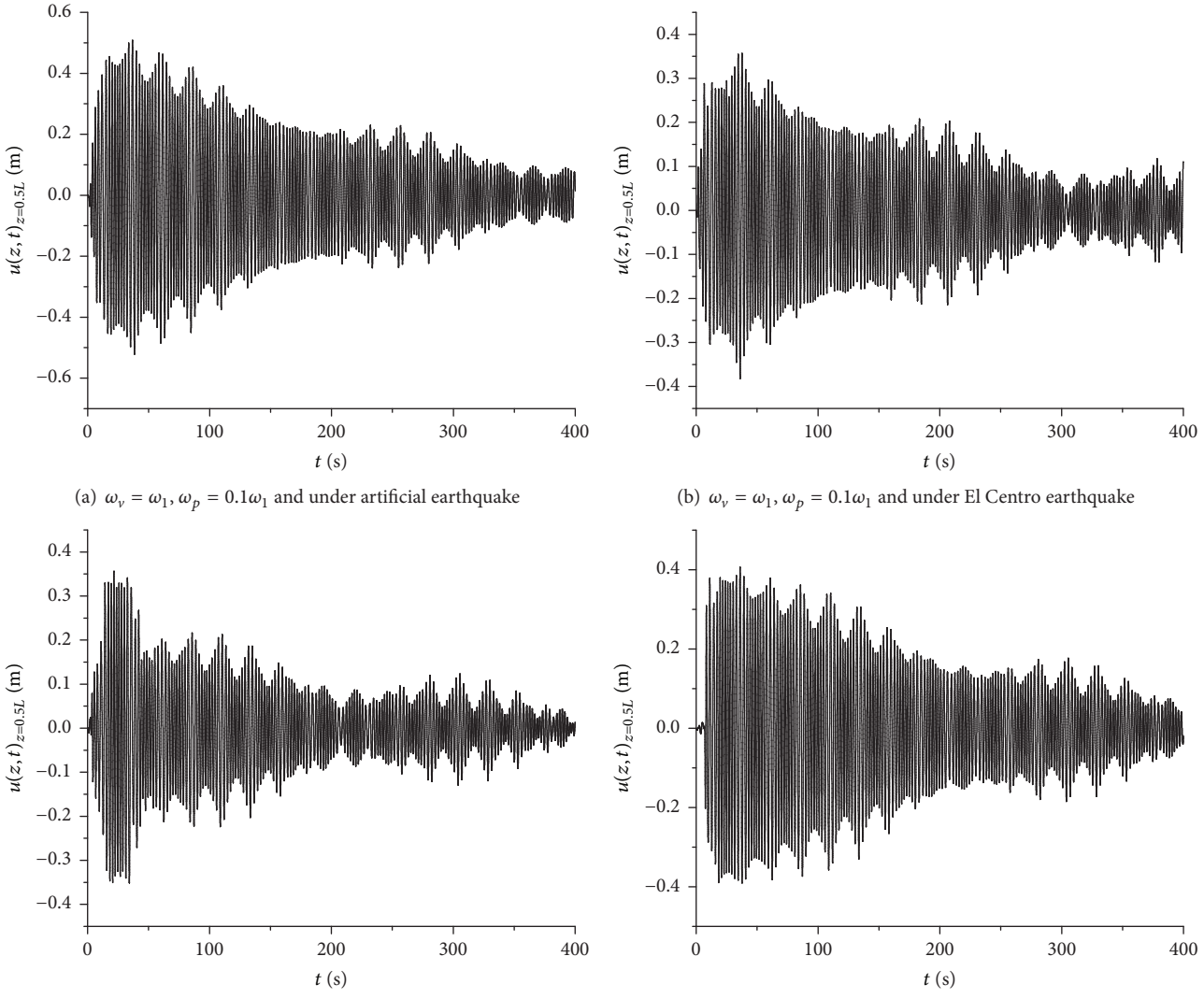

(a) $\omega_v = \omega_1, \omega_p = 0.1\omega_1$ and under artificial earthquake

(b) $\omega_v = \omega_1, \omega_p = 0.1\omega_1$ and under El Centro earthquake

(c) $\omega_v = \omega_1, \omega_p = 0.1\omega_1$ and under Taft earthquake

(d) $\omega_v = \omega_1, \omega_p = 0.1\omega_1$ and under Loma earthquake

Figure 11: Comparison of dynamic responses of the cable between the cases of four site classifications earthquakes.

larger than the other two cases with only combinations of vortex excitation and parametric excitation. Beside, due to the randomness of the earthquake, the curves of dynamic response of the cable become more irregular. Compared with Figure 6(b), due to the effect of earthquake, the maximum value appears at the time of 0~50 s, that is, the time duration of earthquake; after that the motion amplitude attenuates, and the maximum values of dynamic response in Figure 10(a) add from 0.0223 m to 0.221 m. When compared with Figure 7(c), the maximum values of dynamic response in Figure 10(b) add from 0.883 m to 0.916 m, and the maximum value of motion response of the cable appears around from the time point of 50 s to 160 s. It is noted that the earthquake can signally affect the motion amplitude and time points reach the maximum value of the cable. Therefore, dynamic analysis under combined vortex, parametric, and earthquake excitations is necessary.

From Figures 11(a) to 11(d), it can be seen that site class of earthquake wave affects the vibration response of cable largely, and the pattern and motion amplitude of time history of the cable are invariant. The maximum value appears at the time of 0~50 s, that is, the time duration of earthquake; after that the motion amplitude attenuates. In other words, the energy of the dynamic response of the cable is focused on the time duration of earthquake. The difference of seismic wave spectrum characteristics results in the difference of maximum mid-span displacements of the cable. The peak values of the dynamic response of the cable under artificial earthquake, El Centro earthquake, Taft earthquake, and Loma earthquake are 0.522 m, 0.383 m, 0.356 m, and 0.406 m, respectively, and occur at the time that the earthquake wave reaches its energy-intensive zone. Similarly, the root mean square values of the dynamic response of the cable under the above earthquake waves are 0.236 m, 0.156 m, 0.131 m, and 0.202 m, respectively.

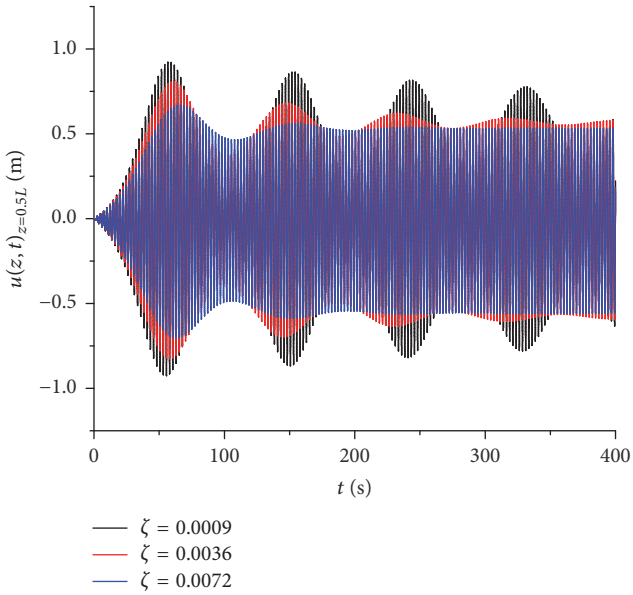

FIGURE 12: The effect of damping ratio on the dynamic response of the cable ($\omega_v = \omega_1$ and $\omega_p = 2\omega_1$).

It is concluded that dynamic response of the cable under artificial earthquake which is suited to rock foundation is the largest. Oppositely, the Taft earthquake which is suited to medium soil foundation induces the smallest dynamic response values of the cable.

3.6. Effect of Damping Ratio. The influence of damping ratio on the dynamic response of the cable is also investigated, and three alternative levels of damping ratio $\zeta = 0.0009, 0.0036, 0.0072$ are adopted. As shown in Figure 12, the motion amplitude and energy of the dynamic response of the cable are decreased as the modal damping ratio is increased. As the damping ratio increases to 0.0072, the wave crests induced by combinations of vortex excitation and parametric excitation are smoothed after the time of 150 s. The rate of descent of the maximum values between $\zeta = 0.0009$ and $\zeta = 0.0072$ is reached up to 72.82%. This is an expected result because damping plays an important role in energy dissipation and makes the cable system more stable [23, 24]. In preliminary design of the cable system, it is recommended that the damping of cable should be increased to reduce the dynamic responses of the system, and large-amplitude vibration of cable may be avoided by locating dampers on the cable or the tube.

3.7. Effect of Lift Coefficient. Based on the work conducted by Chen et al., 2015, the lift coefficient is adopted as a constant value ranging usually from 0.8 to 1.2. As shown in Figure 13, four cases of the cable system under combined excitation are explored to determine the influence of the lift coefficient on the dynamic response, and the three different lift coefficients are $C_L = 0.8, 1.0, 1.2$. When the lift coefficient is ranged from 0.8 to 1.2, the lift coefficient is an important part of the correlated lift force due to vortex shedding; as a consequence, larger lift coefficient can cause larger dynamic response. Thus, the dynamic response of the cable in case of lift coefficient in 0.8 is the smallest while comparing with the case of other constant lift coefficients. As a consequence, larger lift coefficient can cause more unstable dynamic response. In the meanwhile, the inclusion of parametric excitation can strengthen the instability, when it satisfies the special condition which can cause parametric resonance of a cable system. As the effect of self-excitation of nonlinear vortex-induced lift terms, the excitation of resonance becomes weaker, while the lift coefficient is getting lower. In Figure 13(b), the mid-span displacement of the cable is largest, when along axial location, and the maximum amplitude in the case of lift coefficient in 1.2 is more than twice larger than the case of lift coefficient in 0.8.

4. Conclusions

The parametrically excited vibrations of cable of submerged floating tunnel under hydrodynamic and earthquake excitation are studied in this paper. The dynamics motion of the cable is built by Euler beam theory and Galerkin method. Random earthquake excitation in time domain is formulated by trigonometric series method. The hydrodynamic force induced by earthquake excitations is formulated to represent real seaquake conditions. An analytical model is proposed to analyze the cable system for submerged floating tunnel model subjected to combined hydrodynamic force and earthquake excitations. The effects of the hydrodynamic and earthquake parameters and structural parameters on the resulting dynamics response of the system are explored and discussed. The sensitivity of key parameters on the anchor system for submerged floating tunnel is investigated to enable a preliminary examination of the hydrodynamic and seismic behavior of the cable and provide guidance for design and operation of the anchor system for submerged floating tunnel.

The following conclusions can be drawn:

(1) The overall trends of the results obtained by the present method generally agree with the evaluations calculated from the other methods. Due to the seismic design spectrum for offshore structure and the coupled effect of hydrodynamic force and earthquake excitation considered in the present approach, the dynamic responses of the cable are greatly amplified and FFT amplitude component obtained by the present method has more abundant high-frequency contents and excites wider peak frequency region.

(2) The dynamic response of the cable under combinations of vortex excitation and parametric excitation become more complicated, especially in combined resonance condition. Thus, the fundamental frequency of cable of submerged floating tunnel located in complicated marine environment should be thought over carefully to avoid parametric resonance.

(3) Dynamic response of the cable under artificial earthquake which is suited to rock foundation is the largest. Oppositely, the Taft earthquake which is suited to medium soil foundation induces the smallest dynamic response values of the cable.

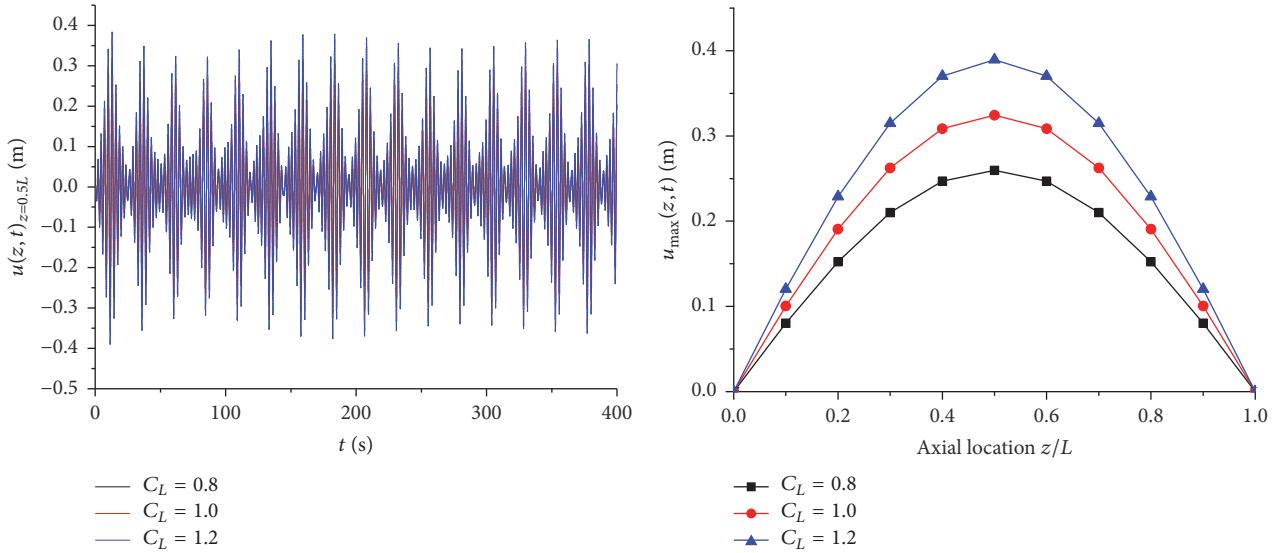

(a) Time history at $\omega_v = \omega_1$, $\omega_p = 0.1\omega_1$

(b) Maximum value of model 1 along axial location

FIGURE 13: The effect of lift coefficient on the dynamic response of the cable.

(4) Damping plays an important role in energy dissipation and makes the cable system more stable. In preliminary design of the cable system, it is recommended that the damping of cable should be increased to reduce the dynamic responses of the system, and large-amplitude vibration of cable may be avoided by locating dampers on the cable or the tube.

Conflicts of Interest

The authors declared no potential conflicts of interest with respect to the research, authorship, and/or publication of this article.

Acknowledgments

This work had been supported by the National Natural Science Foundation of China (Grants nos. 51578164 and 41672296), the China Postdoctoral Science Foundation (Grant no. 2017M610578), the Systematic Project of Guangxi Key Laboratory of Disaster Prevention and Structural Safety (Grant no. 2016ZDX008), and the Innovative Research Team Program of Guangxi Natural Science Foundation (Grant no. 2016GXNSFGA380008).

References

[1] S.-N. Sun, J.-Y. Chen, and J. Li, "Non-linear response of tethers subjected to parametric excitation in submerged floating tunnels," *China Ocean Engineering*, vol. 23, no. 1, pp. 167–174, 2009.

[2] S.-N. Sun and Z.-B. Su, "Parametric vibration of submerged floating tunnel tether under random excitation," *China Ocean Engineering*, vol. 25, no. 2, pp. 349–356, 2011.

[3] W. Lu, F. Ge, L. Wang, X. Wu, and Y. Hong, "On the slack phenomena and snap force in tethers of submerged floating tunnels under wave conditions," *Marine Structures*, vol. 24, no. 4, pp. 358–376, 2011.

[4] S.-I. Seo, H.-S. Mun, J.-H. Lee, and J.-H. Kim, "Simplified analysis for estimation of the behavior of a submerged floating tunnel in waves and experimental verification," *Marine Structures*, vol. 44, pp. 142–158, 2015.

[5] C. Cifuentes, S. Kim, M. Kim, and W. Park, "Numerical simulation of the coupled dynamic response of a submerged floating tunnel with mooring lines in regular waves," *Ocean Systems Engineering*, vol. 5, no. 2, pp. 109–123, 2015.

[6] M. Duan, Y. Wang, Z. Yue, S. Estefen, and X. Yang, "Dynamics of risers for earthquake resistant designs," *Petroleum Science*, vol. 7, no. 2, pp. 273–282, 2010.

[7] R. Dong, X. Li, Q. Jin, and J. Zhou, "Nonlinear parametric analysis of free spanning submarine pipelines under spatially varying earthquake ground motions," *China Civil Engineering Journal*, vol. 41, no. 7, pp. 103–109, 2008.

[8] J. H. Lee, S. I. Seo, and H. S. Mun, "Seismic behaviors of a floating submerged tunnel with a rectangular cross-section," *Ocean Engineering*, vol. 127, pp. 32–47, 2016.

[9] M. Di Pilato, F. Perotti, and P. Fogazzi, "3D dynamic response of submerged floating tunnels under seismic and hydrodynamic excitation," *Engineering Structures*, vol. 30, no. 1, pp. 268–281, 2008.

[10] L. Martinelli, G. Barbella, and A. Feriani, "A numerical procedure for simulating the multi-support seismic response of submerged floating tunnels anchored by cables," *Engineering Structures*, vol. 33, no. 10, pp. 2850–2860, 2011.

[11] Z.-B. Su and S.-N. Sun, "Seismic response of submerged floating tunnel tether," *China Ocean Engineering*, vol. 27, no. 1, pp. 43–50, 2013.

[12] Ministry of Construction, "Code for seismic design of buildings," GB 50011-2010, Ministry of Construction, Beijing, China, 2010.

[13] Z. Su and S. Sun, "Stability of submerged floating tunnel tether subjected to parametric excitation," *Journal of Central South University*, vol. 44, no. 6, pp. 2549–2553, 2013.

[14] S. Lei, W.-S. Zhang, J.-H. Lin, Q.-J. Yue, D. Kennedy, and F. W. Williams, "Frequency domain response of a parametrically excited riser under random wave forces," *Journal of Sound and Vibration*, vol. 333, no. 2, pp. 485–498, 2014.

[15] K. Bi and H. Hao, "Modelling and simulation of spatially varying earthquake ground motions at sites with varying conditions," *Probabilistic Engineering Mechanics*, vol. 29, pp. 92–104, 2012.

[16] International Organization for Standardization (ISO), 2006, Petroleum and Natural Gas Industries-specific Requirements for Offshore Structures-Part 2. Seismic design procedures and criteria, Switzerland.

[17] K. Wang, W. Tang, and H. Xue, "Time domain approach for coupled cross-flow and in-line VIV induced fatigue damage of steel catenary riser at touchdown zone," *Marine Structures*, vol. 41, pp. 267–287, 2015.

[18] T. K. Datta and E. A. Mashaly, "Seismic response of buried submarine pipelines," *Journal of Energy Resources Technology*, vol. 110, no. 4, pp. 208–218, 1988.

[19] J. H. Lee and J. K. Kim, "Dynamic response analysis of a floating offshore structure subjected to the hydrodynamic pressures induced from seaquakes," *Ocean Engineering*, vol. 101, pp. 25–39, 2015.

[20] G. Martire, B. Faggiano, F. M. Mazzolani, A. Zollo, and T. A. Stabile, "Seismic analysis of a SFT solution for the Messina Strait crossing," *Procedia Engineering*, vol. 4, pp. 303–310, 2010.

[21] Z. W. Wu, J. K. Liu, Z. Q. Liu, and Z. R. Lu, "Parametrically excited vibrations of marine riser under random wave forces and earthquake," *Advances in Structural Engineering*, vol. 19, no. 3, pp. 449–462, 2016.

[22] J. Chen, S. Sun, and B. Wang, "Dynamic analysis for the tether of submerged floating tunnel," *Chinese Journal of Computational Mechanics*, vol. 25, no. 4, pp. 487–493, 2008 (Chinese).

[23] W. B. Wu, H. Liu, M. H. El Naggar, G. X. Mei, and G. S. Jiang, "Torsional dynamic response of a pile embedded in layered soil based on the fictitious soil pile model," *Computers and Geotechnics*, vol. 80, pp. 190–198, 2016.

[24] W. Wu, G. Jiang, S. Huang, and C. J. Leo, "Vertical dynamic response of pile embedded in layered transversely isotropic soil," *Mathematical Problems in Engineering*, vol. 2014, Article ID 126916, 12 pages, 2014.